Available online at www.sciencedirect.com

ScienceDirect

IFAC Papers Online CONFERENCE PAPER ARCHIVE

IFAC PapersOnLine 50-1 (2017) 8502–8507

On average real sliding dynamics in linear systems

Josep M. Olm * **Domingo Biel** ** **Víctor Repecho** *** **Yuri B. Shtessel** ****

* *Department of Mathematics & Institute of Industrial and Control Engineering, Universitat Politècnica de Catalunya, 08028 Barcelona, Spain (e-mail: josep.olm@upc.edu)*

** *Institute of Industrial and Control Engineering, Universitat Politècnica de Catalunya, 08028 Barcelona, Spain (e-mail: domingo.biel@upc.edu)*

*** *Institute of Industrial and Control Engineering, Universitat Politècnica de Catalunya, 08028 Barcelona, Spain (e-mail: victor.repecho.del@upc.edu)*

**** *Department of Electrical & Computer Engineering, The University of Alabama in Huntsville, Huntsville, AL 35899, USA (e-mail: shtessy@uah.edu)*

Abstract: It is well known that in implementations of sliding mode controllers using hysteresis comparators, when the hysteresis band amplitude tends to zero the real dynamics tends to the ideal sliding dynamics. However, in real systems physical limitations do not allow to effectively lower this value at will, and a steady state error is likely to appear. In this paper we relate this error with a non zero average value of the switching function in each switching period: it is shown that, in linear systems, when the controller has a constant switching frequency and the switching function is periodic, the average value of the difference between real and ideal steady state dynamics is proportional to the average value of the switching function. Hence, when this average value is non zero an average steady state error appears, while a zero average value for the switching function entails no average steady state error. The proof is carried out using a regular form approach, and the result is exemplified in a buck converter. Simulation results show that when the switching function is periodic and shows a piecewise linear behavior within the hysteresis band, thus guaranteeing zero average value, the average state error disappears. In turn, when this piecewise linear character is lost and the switching function has non zero mean value, an average steady state error arises.

Keywords: Sliding mode control, switching functions, real dynamics, average values

1. INTRODUCTION

In sliding mode control theory, relay implementations of an appropriate control law may constrain the evolution of the system to a pre-defined switching surface, say $s(x) = 0$. The system dynamics therein, obtained through regularization, is known as ideal (sliding) dynamics. Nevertheless, this requires an infinite switching frequency not attainable in physical systems. Hence, practical implementations often use a relay plus hysteresis loop of width, say, 2Δ, that keep the system evolving not on the switching surface but within a boundary layer of the same width around it: these are the real sliding dynamics. It is shown in Utkin (1992) that, in a system with a hysteretic implementation of the control law, for any real solution describing the motion in the boundary layer, there is a solution describing the ideal motion on the switching surface which differs from it within the range of Δ, and when Δ tends to zero the real solutions tend to the ideal solutions.

⋆ Corresponding author: Josep M. Olm (e-mail: josep.olm@upc.edu).

However, physical limitations impose a non zero lower bound for Δ, i.e. do not allow the step $\Delta \to 0$, and classical regularization offers an approximation to the real dynamics with an accuracy depending of Δ. In this paper we take a different approach and propose an additional characterization of the corresponding real dynamics of a linear system with linear switching function, s, by relating its average state value with those of the ideal dynamics and s. Specifically, we show that when the sliding controller works at fixed frequency and the switching function, $s(x(t)) = s(t)$, is periodic, the average value of the difference between "real" and ideal steady states in each switching period is proportional to the average value of the switching function. Hence, when $\langle s \rangle$ is zero, such a steady state average difference is zero as well. This is met, for example, when the switching function shows a piecewise linear behavior within the hysteresis band, this being a key assumption in the fixed frequency implementation scheme proposed in Repecho et al. (2016), and also in the Zero Averaged Dynamics algorithm (ZAD, Fossas et al. (2001)).

10.1016/j.ifacol.2017.08.826

The proof is carried out using a regular form approach (Utkin (1992)).

The theoretical analysis is numerically validated in a buck converter. Simulation results not only confirm the predictions, but show that the average value of the state presents a steady state error with respect to the expected tendency when the piecewise linearity of the switching function within the hysteresis band is not fulfilled. Hence, beyond the key role of the assumption of piecewise linear behavior of the switching function in sliding mode control theory when working on regularization techniques (Utkin (1992)), and that of fixed frequency implementations in power electronics because of its technical advantages (Siew-Chong et al. (2005)), the importance of both hypotheses in practical scenarios is here theoretically supported.

The remainder of the paper is organized as follows. In Section 2, we revise the classical approach in Utkin (1992), and we also provide an alternative, regular-form based analysis of the real sliding dynamics. The main results are stated in Section 3, where an analysis of the average real sliding dynamics in linear system is conducted. A numerical validation is carried out in Section 4 using an ideal buck converter as a case study. Finally, conclusions are drawn in Section 5.

2. PRELIMINARIES

2.1 The classical approach

Consider the linear system

$$\dot{x} = Ax + Bu + g(t), \tag{1}$$

where $x \in \mathbb{R}^n$, $A \in M_n(\mathbb{R})$, $B \in M_{n\times m}(\mathbb{R})$, $g \in \mathbb{R}^n$ is a vector function characterizing external disturbances, and $u \in \mathbb{R}^m$ is the control action vector.

Assume that the hysteretic control law

$$u_i = \begin{cases} u_i^- \text{ if } s_i < -\Delta_i \text{ or } (|s_i| < \Delta_i \text{ and } \dot{s}_i > 0), \\ u_i^+ \text{ if } s_i > \Delta_i \text{ or } (|s_i| < \Delta_i \text{ and } \dot{s}_i < 0), \end{cases} \tag{2}$$

with $\Delta \in \mathbb{R}^+$, and $s = (s_1(x), \ldots, s_m(x))^\top$ being the switching function vector

$$s(x) = Cx, \quad C \in M_{m\times n}(\mathbb{R}),$$

induces a real sliding motion over the intersection of switching hyperplanes $s(x) = 0$. That is, from a certain (finite) time instant the evolution of the system is constrained within the state space region

$$D = \{x \in \mathbb{R}^n;\ \|s(x)\| \le \Delta\},$$

where $\|\cdot\|$ stands for the 2-norm and $\Delta = \sqrt{m}\max\{\Delta_i\}$.

Notice that the control, u, can be expressed as a function of $\dot{s}$ over the trajectories of (1), namely, as

$$\dot{s} = C\dot{x} = C(Ax + Bu + g(t)).$$

Then,

$$u = -(CB)^{-1} C(Ax + g(t)) + (CB)^{-1}\dot{s}, \tag{3}$$

where the non singular character of CB is a necessary condition for an ideal sliding motion to exist on the intersection of switching surfaces $s(x) = 0$. Consequently, this fact is assumed from now on. Taking (3) to (1) yields the real sliding dynamics:

$$\dot{x} = \bar{C}Ax + \bar{C}g(t) + B(CB)^{-1}\dot{s}, \tag{4}$$

where

$$\bar{C} = \mathbb{I}_n - B(CB)^{-1}C. \tag{5}$$

When $\dot{s} = 0$ is imposed, the resulting control in (3) is known as the *equivalent control*, and the corresponding dynamics are the *ideal sliding dynamics*:

$$\dot{x}^* = \bar{C}Ax^* + \bar{C}g(t). \tag{6}$$

It is shown in Utkin (1992) that any solution of the ideal sliding dynamics (6) with asymptotically stable sliding motion on the intersection of the discontinuity surfaces, $s(x) = 0$, will be close to the corresponding solution of the real dynamics (4) within the range of Δ in an infinite time interval that starts at the time instant where sliding mode begins. Notice that in such a case the initial conditions are sufficiently close:

$$\|s(x(0))\| \le \Delta \wedge s(x^*(0)) = 0 \Rightarrow \|C(x(0) - x^*(0))\| \le \Delta,$$

which means that there exists $P \in \mathbb{R}^+$ such that

$$\|x(0) - x^*(0)\| \le P\Delta. \tag{7}$$

In turn, the result can be summarized as

$$\|x(t) - x^*(t)\| \le N\Delta, \text{ with } N \in \mathbb{R}^+, \text{ for any } 0 \le t < \infty,$$

and

$$\lim_{\Delta\to 0} x(t) = x^*(t) \text{ for } 0 \le t < \infty.$$

The proof uses integration by parts and relies on: (a) the bounded characters of both $\|\varphi(t)\|$ and $\int_0^t \left\|\frac{d}{d\tau}\varphi(t-\tau)\right\| d\tau$, where $\varphi(t)$ denotes the transition matrix of (6), namely

$$\varphi(t) = \exp\left(\bar{C}At\right),$$

and (b) the fact that, as $\dot{s} = 0$ on the trajectories of (6) and the sliding dynamics is asymptotically stable by assumption, zero is an eigenvalue of the system matrix $\bar{C}A$ with algebraic and geometric multiplicity equal to m, while the $(n-m)$ remaining eigenvalues correspond to the sliding motion on $s(x) = 0$ and have negative real parts.

2.2 A regular form approach

An alternative way to prove the previous result is by resorting to the *regular form* (Utkin (1992)) of the original system. Essentially, this establishes that there exists a state transformation that recasts (1) as:

$$\dot{x}_1 = A_{11}x_1 + A_{12}x_2 + g_1(t), \tag{8}$$

$$\dot{x}_2 = A_{21}x_1 + A_{22}x_2 + B_1u + g_2(t), \tag{9}$$

while the switching function vector becomes

$$s(x_1, x_2) = C_1x_1 + C_2x_2, \tag{10}$$

where $x_1 \in \mathbb{R}^{n-m}$, $x_2 \in \mathbb{R}^m$, and matrices A_{ij}, C_i, B_i have appropriate dimensions. Moreover, it follows immediately that $CB = C_2B_1$, and the non singularity of CB entails that of the $m \times m$ matrices C_2 and B_1.

Then, the computation of the control from $\dot{s}$ yields:

$$\begin{aligned}\dot{s} =& C_1\dot{x}_1 + C_2\dot{x}_2 = C_1(A_{11}x_1 + A_{12}x_2 + g_1(t)) + \\ &+ C_2(A_{21}x_1 + A_{22}x_2 + B_1u + g_2(t)),\end{aligned}$$

i.e.

$$\begin{aligned}u =& -B_1^{-1}C_2^{-1}C_1(A_{11}x_1 + A_{12}x_2 + g_1(t)) + \\ &- B_1^{-1}(A_{21}x_1 + A_{22}x_2 + g_2(t)) + B_1^{-1}C_2^{-1}\dot{s}.\end{aligned} \tag{11}$$

With this control law the real dynamics is governed by the reduced order system:

$$\begin{aligned}\dot{x}_1 &= A_{11}x_1 + A_{12}x_2 + g_1(t), \\ s &= C_1x_1 + C_2x_2,\end{aligned}$$

i.e.

$$\dot{x}_1 = \left(A_{11} - C_2^{-1}A_{12}C_1\right)x_1 + g_1(t) + C_2^{-1}A_{12}s, \quad (12)$$

$$x_2 = -C_2^{-1}C_1x_1 + C_2^{-1}s. \quad (13)$$

In turn, the ideal dynamics can be obtained setting $s = 0$ in (12),(13):

$$\dot{x}_1^* = \left(A_{11} - C_2^{-1}A_{12}C_1\right)x_1^* + g_1(t), \quad (14)$$

$$x_2^* = -C_2^{-1}C_1x_1^*. \quad (15)$$

Notice that now the input signal in the real dynamics is $s = s(t)$, while in the previous approach it was $\dot{s}$.

Let the ideal sliding dynamics, i.e. that of x_1^*, be asymptotically stable. This means that it is possible to select C_1, C_2 in such a way that

$$A_1 = A_{11} - C_2^{-1}A_{12}C_1 \quad (16)$$

is a Hurwitz matrix: essentially, this requires (A, B) controllable in the original system (see Utkin (1992) for details).

In order to show that the ideal trajectories are close to the real ones within the range of Δ in an infinite time interval, starting when sliding mode begins, we first notice that (7) is still valid for an appropriate value of P, and in particular it entails that

$$\|x_1(0) - x_1^*(0)\| \leq P\Delta, \quad \|x_2(0) - x_2^*(0)\| \leq P\Delta.$$

The solutions of (12) and (14) are, respectively,

$$\begin{aligned} x_1(t) =& e^{A_1t}x_1(0) + \int_0^t e^{A_1(t-\tau)}g_1(\tau)\ dt + \\ &+ \int_0^t e^{A_1(t-\tau)}C_2^{-1}A_{12}s(t)\ dt, \\ x_1^*(t) =& e^{A_1t}x_1^*(0) + \int_0^t e^{A_1(t-\tau)}g_1(\tau)\ dt. \end{aligned}$$

Substracting and taking norms we have that

$$\begin{aligned} \|x_1(t) - x_1^*(t)\| &\leq \left\|e^{A_1t}\right\| \|x_1(0) - x_1^*(0)\| + \\ &+ \int_0^t \left\|e^{A_1(t-\tau)}\right\| \left\|C_2^{-1}\right\| \|A_{12}\| \|s\|\ dt \leq \\ &\leq \left\|e^{A_1t}\right\| P\Delta + \left\|C_2^{-1}\right\| \|A_{12}\| \Delta \int_0^t \left\|e^{A_1(t-\tau)}\right\|\ dt. \end{aligned}$$

The Hurwitz character of A_1 guarantees that both $\left\|e^{A_1t}\right\|$ and $\int_0^t \left\|e^{A_1(t-\tau)}\right\|$ are bounded: the first one by a polynomial with positive coefficients times a decaying exponential, and the second one by a constant plus another polynomial with positive coefficients times the same decaying exponential. Then, there exists a positive value, N_1, such that

$$\|x_1(t) - x_1^*(t)\| \leq N_1\Delta.$$

Moreover, from (13) and (15) it follows that

$$\begin{aligned} \|x_2(t) - x_2^*(t)\| \leq& \left\|C_2^{-1}\right\| \|C_1\| \|x_1(t) - x_1^*(t)\| + \\ &+ \left\|C_2^{-1}\right\| \Delta = N_2\Delta. \end{aligned}$$

Finally, using norm properties,

$$\|x(t) - x^*(t)\| \leq N\Delta, \quad \text{with} \quad N = \max\{N_1, N_2\},$$

for any $0 \leq t < \infty$, and again

$$\lim_{\Delta \to 0} x(t) = x^*(t) \quad \text{for} \quad 0 \leq t < \infty.$$

3. MAIN RESULTS

In real systems, physical limitations do not allow to perform the step $\Delta \to 0$. Thus, according to the previous analysis we can just guarantee $\|x(t) - x^*(t)\| \leq N\Delta$. However, as the switching function vector, s, changes every switching period, a question arises: what is the relation between the average value of the real state, x, in every switching period, and that of the ideal state, x^*?

A rather intuitive answer would be that the relation probably involves the average value of the switching function vector, s, in each switching period. Indeed, implementation techniques such as the ZAD (Ramos et al., 2003) are built on the basis of guaranteeing this zero value for s, this being also ensured by fixed frequency implementations under the assumption of piecewise linear behavior of the switching function vector components (Repecho et al. (2016)).

It is quite evident that in the nonlinear systems case the situation will be non trivial. However, in this paper we just deal with the linear system in regular form analyzed in Subsection 2.2.

Let us define the averaging operator

$$\langle(\cdot)\rangle = \frac{1}{T}\int_{t-T}^{t} (\cdot)\ dt, \quad (17)$$

which is to be computed componentwise in the vector case, and consider the simple but usual situation in which the following assumption is fulfilled:

Assumption A. Once within the boundary layer, both the switching function vector, s, and the disturbance vector, g can be considered T-periodic, $T \in \mathbb{R}^+$, from a certain time instant.

Remark 1. Assumption A is not as restrictive as it might appear. For s, this is met when the hysteresis bandwidth is fixed, in ZAD implementations, and also in regulation problems where fixed frequency is attained via bandwidth adaptation (Repecho et al., 2016). As for g, constant disturbances, for example, fall within this class.

Theorem 1. Consider the real sliding dynamics (12),(13) and the ideal sliding dynamics (14),(15). Let A_1 defined in (16) be a Hurwitz matrix, and let also Assumption A be fulfilled. Then, both systems admit asymptotically stable, T-periodic solutions $\tilde{x}$, $\tilde{x}^*$, respectively, such that

$$\langle\tilde{x}^*\rangle = M^*\langle g_1(t)\rangle, \quad (18)$$

$$\langle\tilde{x}\rangle = \langle\tilde{x}^*\rangle + M\langle s\rangle, \quad (19)$$

where

$$M^* = \begin{pmatrix} -A_1 \\ C_2^{-1}C_1A_1 \end{pmatrix},$$

$$M = \begin{pmatrix} -A_1^{-1}C_2^{-1}A_{12} \\ C_2^{-1}\left(C_1A_1^{-1}C_2^{-1}A_{12} + \mathbb{I}\right) \end{pmatrix}.$$

Corollary 1. If the assumptions of Theorem 1 are fulfilled and $\langle s\rangle = 0$, then $\langle\tilde{x}\rangle = \langle\tilde{x}^*\rangle$, with $\langle\tilde{x}^*\rangle$ given by (18).

Hence, it stems from Theorem 1 that the average value of the ideal steady state solution is proportional to that of the unmatched component of the disturbance, $g_1(t)$. Even more importantly, the difference between the average values of real and ideal steady state solutions is proportional to $\langle s\rangle$. In turn, it is immediate from Corollary 1 that the average values of real and ideal steady state solutions

coincide when the average value of s is zero. This last happens, for example, when working at fixed switching frequency and the switching function components exhibits a piecewise linear behavior within the boundary layer, as depicted in Figure 1.

Proof. As A_1 is Hurwitz and Assumption A is fulfilled, the existence of T-periodic, asymptotically stable solutions $\tilde{x}^\top = \left(\tilde{x}_1^\top, \tilde{x}_2^\top\right)$, $\tilde{x}^{*\top} = \left(\tilde{x}_1^{*\top}, \tilde{x}_2^{*\top}\right)$ for (12),(13) and (14),(15), respectively, is ensured by basic linear systems theory (Teschl (2012)). In turn, these solutions satisfy:

$$\dot{\tilde{x}}_1 = A_1\tilde{x}_1 + g_1(t) + C_2^{-1}A_{12}s, \tag{20}$$

$$\tilde{x}_2 = -C_2^{-1}C_1\tilde{x}_1 + C_2^{-1}s, \tag{21}$$

and

$$\dot{\tilde{x}}_1^* = A_1\tilde{x}_1^* + g_1(t), \tag{22}$$

$$\tilde{x}_2^* = -C_2^{-1}C_1\tilde{x}_1^*. \tag{23}$$

Applying the averaging operator (17) to (20),(22) while taking into account its linearity and the fact that $\left\langle \dot{\tilde{x}}_1 \right\rangle = 0$, $\left\langle \dot{\tilde{x}}_1^* \right\rangle = 0$, because neither $\dot{\tilde{x}}_1$ nor $\dot{\tilde{x}}_1^*$ have continuous component but just zero average terms, it results that

$$0 = A_1 \left\langle \tilde{x}_1 \right\rangle + \left\langle g_1(t) \right\rangle + C_2^{-1}A_{12} \left\langle s \right\rangle,$$
$$0 = A_1 \left\langle \tilde{x}_1^* \right\rangle + \left\langle g_1(t) \right\rangle.$$

Then, it follows immediately from the Hurwitz character of A_1 that

$$\left\langle \tilde{x}_1^* \right\rangle = -A_1^{-1} \left\langle g_1(t) \right\rangle,$$
$$\left\langle \tilde{x}_1 \right\rangle = \left\langle \tilde{x}_1^* \right\rangle - A_1^{-1}C_2^{-1}A_{12} \left\langle s \right\rangle$$

and, subsequently from (21),(23),

$$\left\langle \tilde{x}_2^* \right\rangle = C_2^{-1}C_1A_1^{-1} \left\langle g_1(t) \right\rangle,$$
$$\left\langle \tilde{x}_2 \right\rangle = \left\langle \tilde{x}_2^* \right\rangle + C_2^{-1} \left(C_1A_1^{-1}C_2^{-1}A_{12} + \mathbb{I} \right) \left\langle s \right\rangle.$$

Now, gathering terms appropriately, (18),(19) follow immediately. As for Corollary 1, it is straightforward. □

Remark 2. The same results can be drawn from the formulation (4),(6). However, the singularity of the system matrix complicates somehow the discussion. Indeed, as $\tilde{C}A$ has m distinct zero eigenvalues and $n-m$ eigenvalues with negative real part, when $\langle s \rangle = 0$ it has to be shown that the intersection of the null spaces of C and $\tilde{C}A$ only contains the zero vector; this can be done through a state transformation that yields an appropriate decoupling of the system matrix, which in fact resorts to the regular form. Instead, when $\langle s \rangle \neq 0$, the first set of m equations are to be replaced bt $C \langle x \rangle = \langle s \rangle$, and then one has to play with the remaining $n-m$ equations. In any case, the regular form allows an easy obtaining of explicit expressions for both situations.

Remark 3. The T-periodicity of s and g required in Assumption A is essential for the ideal and real sliding dynamics to show T-periodic solutions. If any of these is not fulfilled, the result is no longer valid.

4. CASE STUDY: THE BUCK CONVERTER

4.1 Mathematical model

Consider the following normalized model of an ideal buck converter:

$$\dot{x}_1 = -x_2 + \beta u, \tag{24}$$

$$\dot{x}_2 = x_1 - \gamma x_2, \tag{25}$$

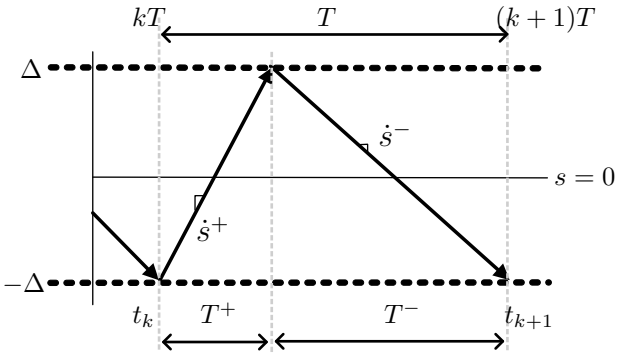

Fig. 1. Piecewise linear behavior of a switching function, $s(x)$, in the vicinity of the switching surface $s(x) = 0$.

where x_1 and x_2 are proportional to the inductor current and the output voltage, respectively, $u \in \{0, 1\}$ is the control action, and β, γ are real, positive values depending on the system parameters.

It is easy to show that the control law (2) with $u^+ = 1$ and $u^- = 0$, with $\Delta \in \mathbb{R}^+$, and $s = s(x)$ being the switching function

$$s(x) = \alpha\left(\bar{x}_2 - x_2\right) + \frac{d}{dt}\left(\bar{x}_2 - x_2\right), \quad \alpha \in \mathbb{R}^+, \tag{26}$$

where $\bar{x}_2 \in \mathbb{R}^+$ stands for a constant voltage reference, confines the evolution of the system to the state space region

$$D = \left\{ x \in \mathbb{R}^2;\ |s(x)| \leq \Delta \right\},$$

from a certain time instant. It is worth remarking that the switching function (26) yields a robust regulation of the x_2 state variable, i.e. of the output voltage (Bilalović et al., 1983).

Defining the error variable $e = (e_1, e_2)^\top$, with

$$e_1 = \gamma\bar{x}_2 - x_1, \quad e_2 = \bar{x}_2 - x_2, \tag{27}$$

the error dynamics read as

$$\dot{e}_1 = -e_2 + \bar{x}_2 + \beta u, \tag{28}$$

$$\dot{e}_2 = e_1 - \gamma e_2, \tag{29}$$

and the switching function becomes

$$s(e_1, e_2) = e_1 + (\alpha - \gamma)\, e_2. \tag{30}$$

System (28),(29) is already in regular form and matches (8),(9), and so does the switching function (30) with (10). Hence, following the procedure in Section 3, the real dynamics (12),(13) reads now as

$$e_1 = (\gamma - \alpha)\, e_2 + s, \tag{31}$$

$$\dot{e}_2 = -\alpha e_2 + s, \tag{32}$$

while the ideal dynamics (14),(15) boils down to

$$e_1^* = (\gamma - \alpha)\, e_2^*, \tag{33}$$

$$\dot{e}_2^* = -\alpha e_2^*. \tag{34}$$

Notice that, in this case, $g(t) = 0$ and $\alpha > 0$; consequently, when $s = s(t)$ is T-periodic within D the hypotheses of Theorem 1, including Assumption A, are fulfilled. Hence, the solutions of (31),(32) tend asymptotically to the periodic solution $\tilde{e} = (\tilde{e}_1, \tilde{e}_2)^\top$, with $\tilde{e}_1, \tilde{e}_2$ related by (31). As for $\tilde{e}_2$, a T-periodic solution for (32) is given by (see, for example, Lewis (2003)):

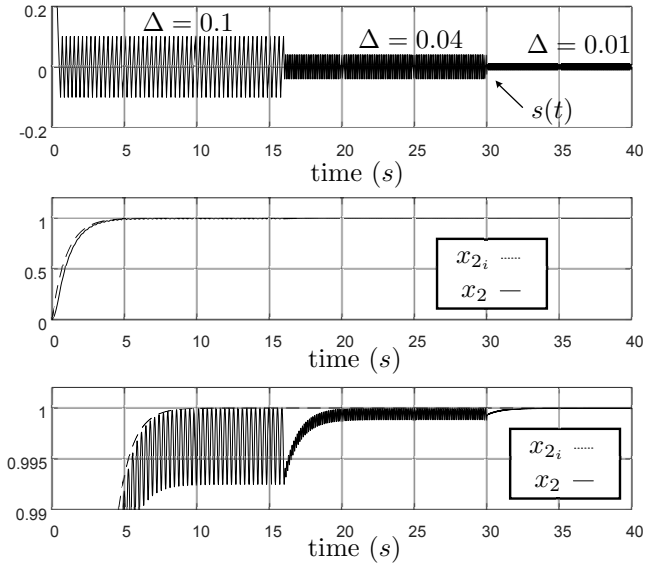

Fig. 2. System response whit different hysteresis band values. Top: switching function. Mid: state variable x_2 and its reference, $\bar{x}_2$. Bottom: zoom of the mid plot.

$$\tilde{e}_2(t) = \frac{e^{-\alpha t}}{e^{\alpha T} - 1} \int_0^T e^{\alpha \tau} s(\tau)\, \mathrm{d}\tau + e^{-\alpha t} \int_0^t e^{\alpha \tau} s(\tau)\, \mathrm{d}\tau. \tag{35}$$

In turn, the solutions of (33),(34) tend asymptotically to the equilibrium point $\tilde{e}^* = 0$.

Then, according to Theorem 1, (18) becomes $\langle \tilde{e}^* \rangle = 0$, while $\langle \tilde{e} \rangle$ is fulfilling (19), i.e.

$$\langle \tilde{e}_1 \rangle = \gamma \langle s \rangle, \tag{36}$$

$$\langle \tilde{e}_2 \rangle = \frac{1}{\alpha} \langle s \rangle. \tag{37}$$

Furthermore, in case that $\langle s \rangle = 0$, (36),(37) yield $\langle \tilde{e} \rangle = \langle \tilde{e}^* \rangle = 0$, thus concurring with the prediction of Corollary 1 for this system.

4.2 Simulation results

A numerical analysis of system (24),(25) has been carried out with parameter values $\beta = \gamma = 3$. For the switching surface (26) we have chosen $\alpha = 1$, while the reference value for x_2 has been set to $\bar{x}_2 = 1$. In accordance with (27), this selection entails that the ideal steady-state value for x_1 is 3.

The simulation consists in implementing the control law described in the previous Subsection with three different values for the hysteresis bandwidth,

$$\Delta = \begin{cases} 0.1 & \text{when} \quad 0 \le t < 16s, \\ 0.04 & \text{when} \quad 16s \le t < 30s, \\ 0.01 & \text{when} \quad 30s \le t < 40s, \end{cases}$$

and checking that (36),(37) are fulfilled, i.e. that the average steady state errors $\langle e_1 \rangle$, $\langle e_2 \rangle$ verify:

$$\langle e_1 \rangle = 3 \langle s \rangle, \quad \langle e_2 \rangle = \langle s \rangle.$$

For, we will assume that during the last instants of the time windows in which each of the three values of Δ is active the variables have achieved a steady state.

The tests have carried out with the software package MATLAB/Simulink (R2016b) using an ODE 5 solver with a fixed step of 10^{-5}. As for the average values, they have been extracted using a low-pass filter with transfer function

$$H(s) = \left(\frac{100}{s^2 + 18s + 100} \right)^{10}.$$

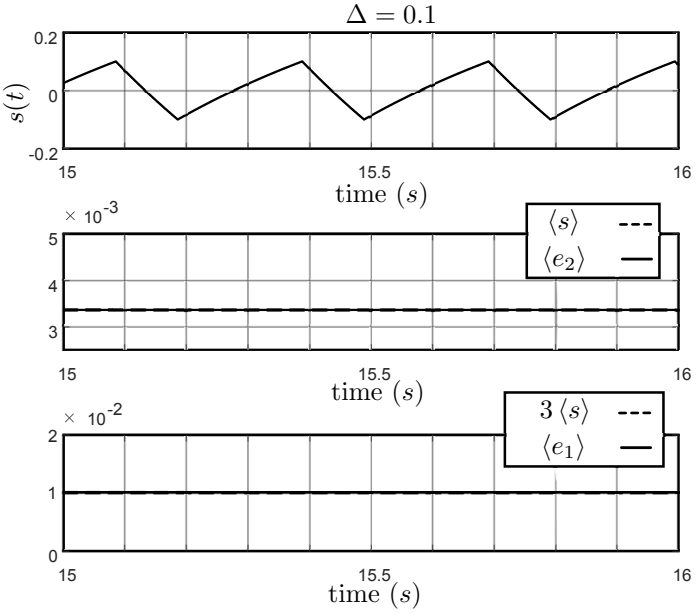

Fig. 3. Performance for $\Delta = 0.1$ in the steady state. Top: switching function. Mid: $\langle e_2 \rangle$ matching $\langle s \rangle$. Bottom: $\langle e_1 \rangle$ matching $3 \langle s \rangle$.

The top plot in Figure 2 depicts the switching function, $s(t)$. As expected, the chattering amplitude is higher when $\Delta = 0.1$, and decreases while Δ does. In turn, the mid plot depicts the behavior of the state variable x_2 with respect to its reference value. The zoom in the bottom plot reveals that x_2 stabilizes closer to the reference, i.e. with less average steady-state error, and also with decreasing chattering amplitude, for lower values of Δ.

This behavior of x_2 can be explained in terms of the average value of the switching function. The top plots in Figures 3, 4 and 5 show the switching surface and its mean value for $\Delta = 0.1$, $\Delta = 0.04$ and $\Delta = 0.01$. Notice that the signal envelope allows an easy identification of the current hysteresis value. It is also worth emphasizing that, as we are in a regulation control problem and the hysteresis band is symmetric with respect to zero, the switching period of the control action achieves a constant value, T, in the steady state, and the switching function becomes T-periodic, thus meeting one of the hypotheses in Section 3.

It is clear from the top plot in Figure 3 that, for the highest value of the hysteresis, namely $\Delta = 0.1$, the switching function does not show a piecewise linear behavior. Consequently, its mean value is not zero, as confirmed by the mid plot, where it is shown to match that of e_2, this resulting in the steady state error for x_2 observed in the first part of the bottom plot in Figure 2. In turn, one can observe in Figures 4 and 5 that lower values of Δ enforce the piecewise linear character of s within the hysteresis band, this yielding lower mean values for the respective

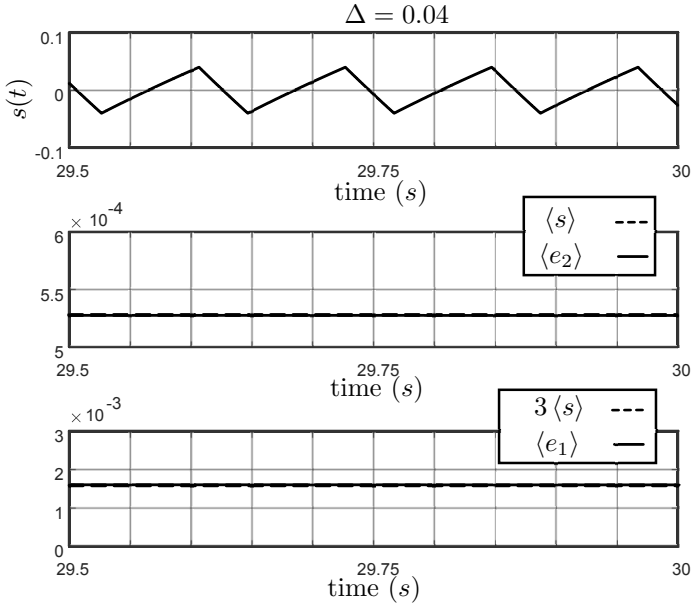

Fig. 4. Performance for $\Delta = 0.04$ in the steady state. Top: switching function. Mid: $\langle e_2 \rangle$ matching $\langle s \rangle$. Bottom: $\langle e_1 \rangle$ matching $3\langle s \rangle$.

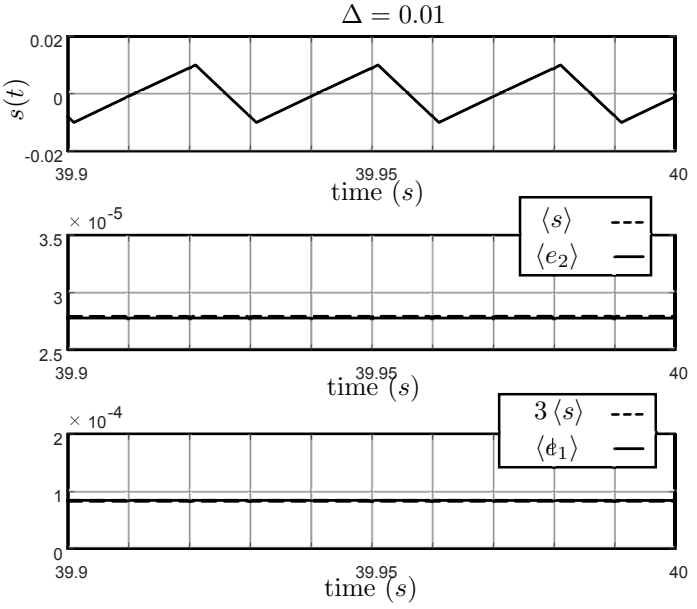

Fig. 5. Performance for $\Delta = 0.01$ in the steady state. Top: switching function. Mid: $\langle e_2 \rangle$ matching $\langle s \rangle$. Bottom: $\langle e_1 \rangle$ matching $3\langle s \rangle$.

switching functions and also for the steady state errors of x_2 arising in Figure 2. In all these cases $\langle e_2 \rangle$ matches $\langle s \rangle$. In turn, $\langle e_1 \rangle$ always coincides with $3\langle s \rangle$, as expected.

Hence, this confirms the theoretical predictions of Section 3. When the piecewise linear assumption for $s(x)$ is closer to be fulfilled, the average values of s tend to zero, and so do the average state errors, $\langle e_1 \rangle$, $\langle e_2 \rangle$. Conversely, steady-state errors appear in the state variables when the piecewise linear assumption for $s(t)$ does not hold and $\langle s \rangle \neq 0$. In any case $\langle e_1 \rangle$, $\langle e_2 \rangle$, match the expected values $3\langle s \rangle$ and $\langle s \rangle$, respectively.

5. CONCLUSIONS

In this paper we showed that, in linear systems with hysteretic implementations of sliding mode controllers, once the switching function is periodic and lies within the hysteresis band, the average difference between the "real" and the ideal steady state sliding dynamics is proportional to the average value of the switching function. Hence, when this average is zero, as happens when the switching function exhibits a piecewise linear behavior and the hysteresis band is symmetric with respect to the switching surface, so is the average difference of real and ideal steady state dynamics. The result was verified both analytically and numerically using a buck converter.

Further research will be devoted to experimentally validate this result, as well as to study an eventual extension of it to the nonlinear case.

ACKNOWLEDGEMENTS

D. Biel, J.M. Olm and V. Repecho are partially supported by the spanish Ministerio de Educación project DPI2013-41224-P and the catalan AGAUR project 2014 SGR 267.

REFERENCES

Bilalović, F., Musić, O., and Sabanović, A. (1983). Buck converter regulator operating in the sliding mode. In *Proc. VII Internat. Conf. on Power Conversion (PCI)*, 331–340.

Fossas, E., Griñó, R., and Biel, D. (2001). Quasi-Sliding control based on pulse width modulation, zero averaged dynamics and the L2 norm. In X. Yu and J. Xu (eds.), *Advances in Variable Structure Systems. Analysis, integration and applications*, 335–344. World Scientific.

Lewis, A. (2003). *A Mathematical Approach to Classical Control*. Queens University.

Ramos, R., Biel, D., Fossas, E., and Guinjoan, F. (2003). A fixed-frequency quasi-sliding control algorithm: application to power inverters design by means of FPGA implementation. *IEEE Trans. Power Electronics*, 18, 344–355.

Repecho, V., Biel, D., Olm, J., and Fossas, E. (2016). A fixed-frequency quasi-sliding control algorithm: application to power inverters design by means of FPGA implementation. *IEEE Trans. Power Electronics, in press*.

Siew-Chong, T., Lai, Y., Cheung, M., and Tse, C. (2005). On the practical design of a sliding mode voltage controlled buck converter. *IEEE Trans. Power Electronics*, 20, 425–437.

Teschl, G. (2012). *Ordinary differential equations and Dynamical Systems*, volume 140 of *Graduate Studies in Mathematics*. American Mathematical Society.

Utkin, V. (1992). *Sliding Modes in Control Optimization*. Springer-Verlag.